



A Brief Review of Electron beam melting (EBM) manufacturing of Ti-6Al-4V alloy for biomedical applications

Ali Talib Khanjar¹, Nuha Hadi Jasim Al Hasan^{1*}

¹Department of Engineering Materials, college of engineering, University of Basra, Basra, Iraq

Received: 1 Feb 2024; Revised: 15 Feb 2024; Accepted for publication: 10 March 2024

* Corresponding author: nuha.jasim@uobasrah.edu.iq

© Published by Shahid Chamran University of Ahvaz.

Abstract

The The aim Electron beam melting (EBM) is a rapidly evolving additive manufacturing (AM) technology demonstrating immense potential for biomedical applications due to its ability to fabricate complex and high-performance metal components. This review critically examines the current state of EBM for biomedical alloys, focusing on key aspects like material compatibility, process parameters, microstructure and mechanical properties, post-processing, and biological performance. We analyze the advantages and limitations of EBM compared to other AM and traditional manufacturing techniques for medical devices, highlighting its unique capabilities in producing lattice structures and patient-specific implants. Finally, we explore the latest advancements in EBM technology, including novel materials, multi-material printing, and in-situ monitoring, emphasizing their potential for further revolutionizing the field of biocompatible implants and medical devices.

Keywords: Ti-6Al-4V alloy; Laser powder bed fusion; Electron beam melting; Microstructure; Biomedical behavior

1. Literature Survey

With additive manufacturing (AM), complex geometries and structures can be fabricated from 3D model data. A digitally defined heat source melts or fuses powder or wire feedstock and then solidifies it after it has solidified, as opposed to subtractive manufacturing processes. By using this technology, manufacturing time can be minimized, which can improve the efficiency of creating new products. The additive manufacturing process is a method of making 3D components from CAD data by depositing material layer by layer, with the use of a 3D printer [1], [2]. Bourell et al. [3] mapped the future of AM, pinpointing key areas for progress: design, process control, materials & machines, biomedical applications, and sustainability. There is a wide variety of metallic and non-metallic materials that can be printed today [4], [5]. The materials that can currently be manufactured using AM technology include ceramics, concrete, polymer powders, acrylonitrile butadiene styrene (ABS), wax, metals, adhesive-coated sheets, and poly-lactic acid (PLA) [1].

1.1 Classification of AM

There are several ways to classify AM processes, including the type of material, the method of solidification, and the way it is deposited [6], [7]. It's important to consider that each technique has both weak and strong points. Hence, the fabrication cost, time, and accuracy of an AM process should be taken into account when choosing the right technology for a particular application. The diagram in **Fig. 1** breaks down AM technologies by their materials, processes, and printing order.

The traditional prototyping process involves removing material from the initial product in order to create final one. As opposed to rapid prototyping, which builds the desired product layer by layer, rapid prototyping makes use of material added layer by layer [1], [8]. There are various methods of manufacturing components by deforming or removing material, such as turning, grinding, milling, and coining. Today, forging, machining, and other subtractive manufacturing methods are most common. However, a significant amount of material waste is generated by subtractive manufacturing processes. The process of additive manufacturing increases material utilization and produces components with near-net shapes [1], [9]. Likewise, AM can be used to fabricate implants and medical devices due to its dimensional stability and ability to

customize [10]. The AM process is less expensive than conventional manufacturing for small-batch production, but it is still an expensive investment compared to conventional manufacturing [1], [3], [9].

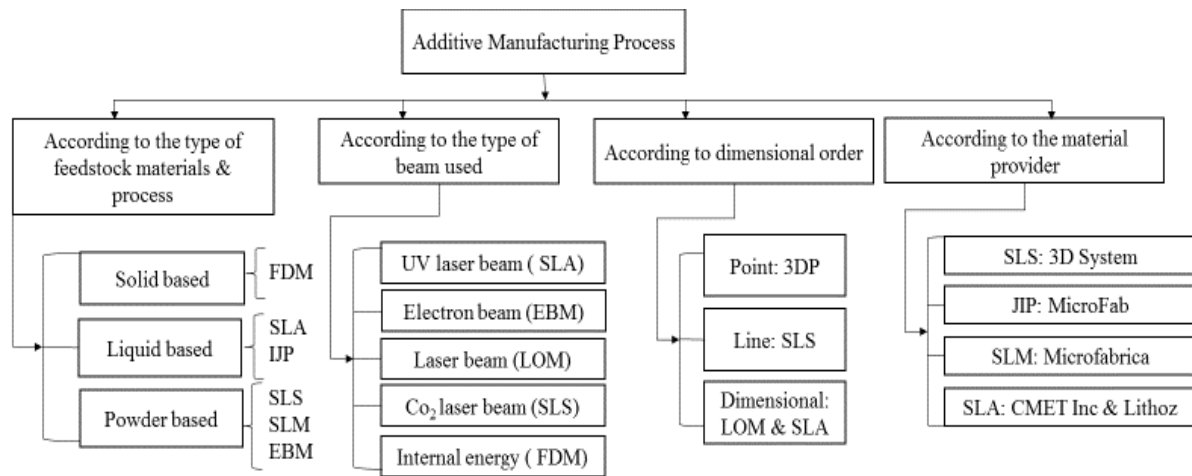


Fig. 1 Classification of additive manufacturing [1]

Furthermore, the material used in AM technologies should be prepared in a way that is compatible with the process (for instance, powder, sheet, wire, or liquid). For example, feedstock for vat polymerization and photopolymer jetting must be thermoset plastic monomers that crosslink under electromagnetic radiation [11]. Components made with additive manufacturing can be made from ceramics, polymers, metals, plastics, or any combination of these materials [1], [7], [12], [13].

1.2 Electron beam melting

Powder bed fusion, a popular AM technique, utilizes lasers or electron beams to melt and bond powder layers, building objects layer by layer [14]. After each powder layer is laid down, the material is fused repeatedly, building the 3D part layer by layer. This process, known as powder bed fusion, can be achieved through various methods like SLM, SLS, DMLM, and EBM. However, sintering isn't ideal for high-density metal powders [14], [15].

Electron beam melting is expected to revolutionize industrial production due to its ability to layer metallic components from computer-aided design data on a powder bed using a high-power electron beam. The microstructure of EBM-produced components differs significantly from those produced by traditional metallurgical techniques due to micro-zone melting. The EBM process involves controlling the electron beam using electromagnetic lenses, allowing for scanning velocities of up to 10^5 m/s on the powder bed. SLM systems have more defects than EBM systems in vacuum environments. A computer builds the 3D model and slices it into

thin layers before being scanned layer by layer by the EBM system until the building process is complete [16], [17].

The Arcam1 EBM system is illustrated in **Fig. 2**. Metallic powder is stored in powder cassettes and gravity causes, it is raked into the building plate by the chamber plate as it falls, forming an approximately 50- μ m-thick powder layer. Electron guns emit electron beams with voltages of 60 kV and currents of 1-50 mA, which produce peak beam powers of approximately 3 kW. In this machine, a laser beam is focused on the powder bed and a beam deflection coil is used to scan and melt the powder that is on the part controlled by a computer. During EBM, titanium and aluminum alloys have a high affinity for gases, so oxygen and nitrogen are not allowed to react with them in a vacuum chamber. Building chambers are introduced with helium gas at 10^3 mbar pressure in order to prevent smoke from forming. Every layer of the sample is preheated, melted, dropped, and a new powder layer is deposited. Within the machine chamber, the samples are cooled to room temperature after the final layer is completed, which normally takes over 2 hours in a helium atmosphere [16].

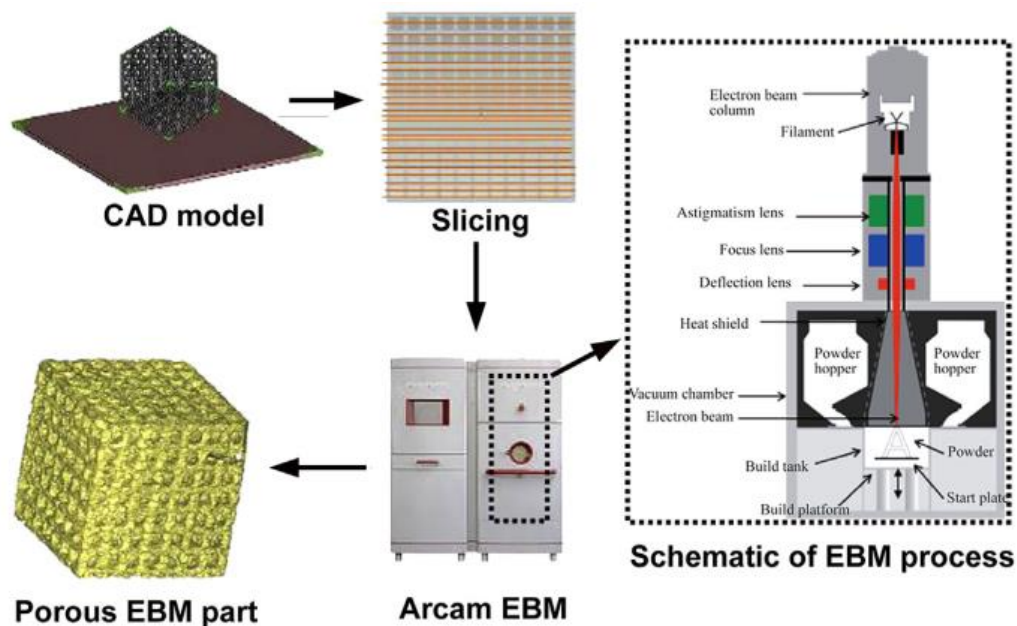


Fig. 2 Schematic diagram of EBM system from design to obtaining final product [16]

Layers are built up to build the component. Four steps are involved in generating each layer, as shown in **Fig. 2 & 3**. After the last layer has been completed, the component inside the machine will cool down. The process chamber is usually flooded with helium to accelerate cooling [17].

The upper section of an EBM system consists mainly of the column, and the lower section consists mainly of the work chamber. EBM was developed by Arcam AB in 1963. Tungsten

filaments or LaB6 crystals are electrochemically activated by 60 kV anodic potential applied to the column. 10–40% of the speed of light is used to guide electrons as they accelerate towards the working chamber. Electromagnetic lenses, also called coils, control the EB. First, astigmatic lenses maintain electron beam shape and deflection; second, focus lenses, control beam focus and third, defect lenses, control beam size. A small mass electrostatically accelerated electron has a lot of kinetic energy when it hits a powder bed. This kinetic energy is converted into heat. Metal particles melt under the influence of this energy. EBs are used instead of defocused beams for preheating powder beds for EBM. As the powder bed is sintering, heat is more easily conducted during the preheating phase. Ti-6Al-4V alloy is typically preheated between 650 and 700 °C. EBM is a hot process. Due to preheating before melting and the vacuum environment, the chamber's working temperature is approximately the same as the preheating temperature. There is low thermal shrinkage in this particular powder bed, and there is a medium amount of sintering between the particles [18].

To construct the component, layers are added one after another. Each layer is generated in four steps (see **Fig 3**). The component is cooled down within the machine after the last layer is completed. The process chamber is normally flooded with helium to accelerate cooling.

Arcam AB developed two main components: an upper column and a lower work chamber. In a column in which a 60 kV anodic potential is applied, an EB is produced by tungsten filaments or LaB6 crystals. Electrons are accelerated up to 10–40% of the speed of light and guided towards the working chamber from the top gun. There are three sets of coils, also known as electromagnetic lenses, that control the EB. Electron beams are shaped and defective in the first set of coils (astigmatic lenses), focused in the second set (focus lenses), and sized in the last set (defect lenses). In spite of their small mass, electrons' kinetic energy is converted into heat when they impact a powder bed. The melting of metallic particles is ensured by this energy. In contrast to the other PBF processes, the EBM process starts with preheating the powder bed using a defocused EB, high beam current, and speed values. Sintering and heat conduction are facilitated during the preheating phase. Ti-6Al-4V alloys typically require preheating at 650–700°C. EBM is a hot process. The working temperature is approximately the same as the preheating temperature since the chamber is vacuum-conditioned and preheated before melting. In this way, small thermal shrinkages are avoided and a medium grade of sintering is achieved, resulting in a powder bed with a specific strength [18].

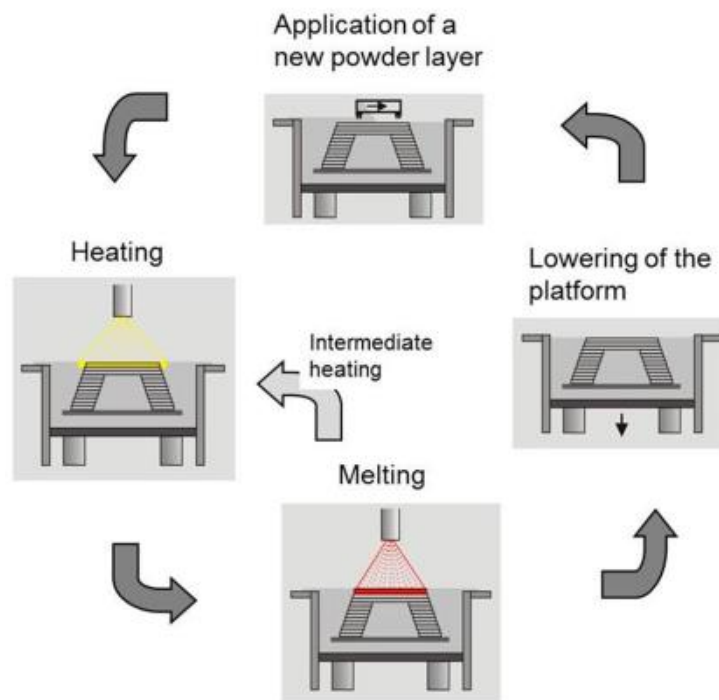


Fig. 3 Four steps of building a layer in EBM method [17]

The initial step involves using a stainless-steel rake to apply a thin layer of powder onto the building area, with the maximum size depending on the machine and typically around 250 mm x 250 mm. The powder is supplied from two magazines located above the building plane, and the thickness of the layer is determined by the desired layer thickness, which typically ranges from 50 to 150 μm . The first layer is applied onto a preheated start plate, usually made of stainless steel, with the preheating temperature slightly above the building temperature. To avoid contamination, it is recommended that the plate material and the building material be similar or the same. The powder's flowability, characterized by its apparent density and tap density, should be as high as possible, and spherical gas atomized powders are commonly used with a recommended size range of 40 to 105 μm . Powders with a smaller mean diameter can cause process instabilities, while larger ones can still be used. It is best to minimize the fraction of smaller particles and small satellites to maintain flowability, density, and electric conductivity [17].

The heating process involves the use of an electron beam to scan the applied powder multiple times across the layer. This step serves two important purposes: to maintain the temperature within the building volume (T_B) by delivering energy, and to slightly sinter the powder particles. The latter is crucial for enhancing the electric conductivity of the powder and preventing process instabilities such as "smoke", which can cause the powder to disperse within

the machine due to repulsion of charged particles. The defocused electron beam used for heating scans the building area several times at velocities of approximately 10 m/s, while the beam power (P) is progressively increased to around 3 kW (**Fig. 4a**). Preheating temperatures and strategies depend on both the metal or alloy and the powder properties. T_B , which is measured using a thermocouple at the starting plate, typically ranges from 300 °C for pure copper to 1100 °C for intermetallic phases or some nickel-base alloys. If the powder contains a high fraction of fine particles, preheating must be done with great care to avoid smoke. Remaining microstructure and stresses are significantly affected by high building temperatures. Due to reduced cooling velocities and temperature gradients, EBM produces lower residual stresses and coarser microstructures than laser-based AM processes [17].

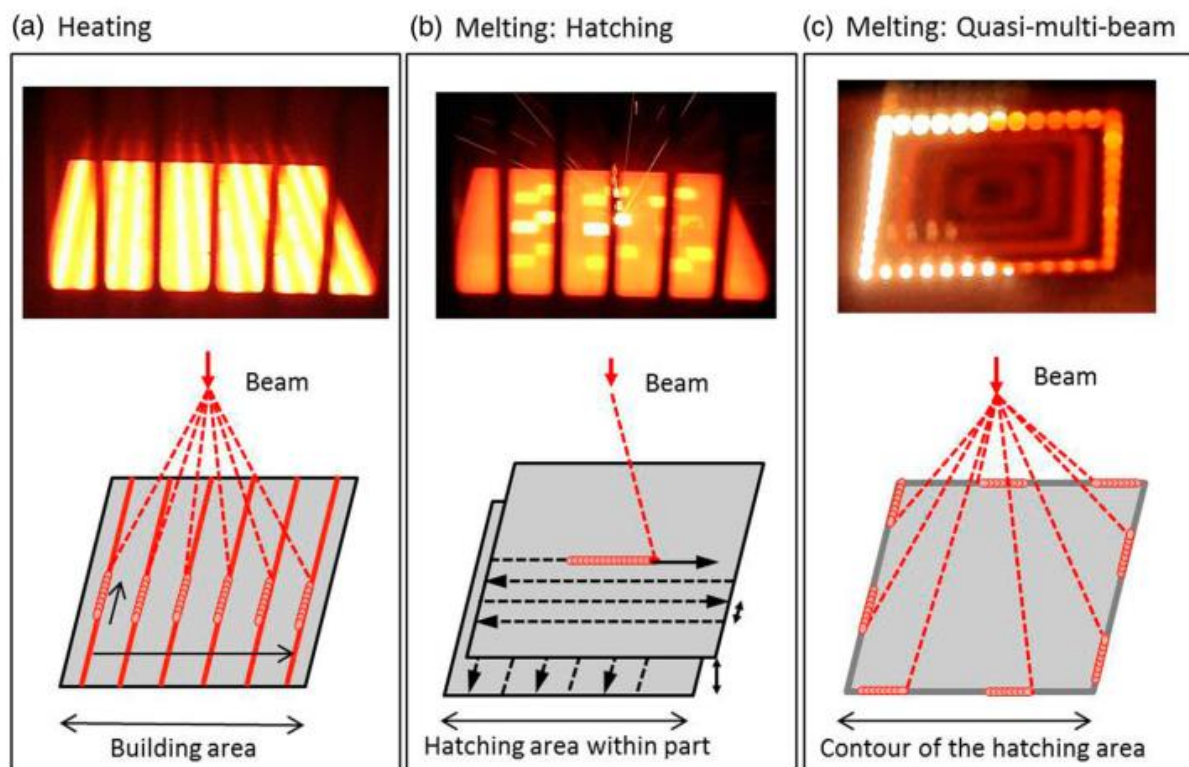


Fig. 4 During EBM, heat and melting occur. At the top: photograph during the process. A schematic representation of beam movement is shown at the bottom: (a) heating with a defocused beam scanning the entire building area, (b) melting by hatching, and (c) contour melting by jumping between points. [17].

A preheated powder layer is scanned with a lower velocity electron beam (typically 4 m/s) that melts the powder particles into a solid material (**Fig. 4b**). Differentiation of melting of areas and contours requires a variety of process parameters, including beam power P , beam velocity

v, distance between lines d , focus offset of the beam, and contour number. Melting of areas is generally achieved through hatching, where the beam direction changes in each line and also in each layer by 90° . With EBM, contours can also melt in a quasi-multi-beam mode, where up to 100 points can be melted simultaneously by jumping from one point to another, which is applied to increase surface quality and reduce roughness (**Fig. 4c**) [17].

1.3 EBM of Ti alloy

The EBM process is versatile and can be applied to various material classes. However, the current use of this technology is mainly focused on titanium and its alloys. Traditionally, titanium parts were produced through forging, extrusion, or casting. However, these processes faced several challenges due to the high melting temperature, low fluidity, and susceptibility to atmospheric agents. In conventional manufacturing processes, complex geometries were difficult to make due to their high cost. The high power and vacuum environment of EBM technology makes these materials increasingly useful [25].

Generally, casting methods do not yield homogeneous compositions because they require removing HDI and LDI when melting Ti-6Al-4V. A high degree of surface oxidation is also an issue with this alloy, particularly at high temperatures. Scientists have explored alternative methods of fabricating components from this alloy to overcome these challenges. With additive manufacturing (AM), high-quality titanium components can be produced with fewer defects than traditional manufacturers [18].

Using electron beam melting (EBM) and direct energy deposition (DED), titanium additive manufacturing began in 1997 with Aeromet Corporation and Arcam AB. Initially, the focus was on producing expensive aerospace and medical components. Other companies, such as EOS, Concept Lasers, MTT, SLM Solutions, Sciaky, and Solidica, soon joined the effort. **Table 1** compares the capabilities, benefits, and limitations of different AM technologies for titanium parts. SLM and EBM offer better surface finish and smaller layer thickness, making them suitable for accurate and complex small objects. DMD, on the other hand, is better for building larger parts at a higher processing rate, albeit with a coarser surface finish [19].

Titanium and its alloys are the focus of EBM research, particularly Ti-6Al-4V. Because EBM is almost completely vacuum-sealed, it has a near-perfect resistance to contamination by gases, especially oxygen [17]. The cost of titanium materials is high and difficult to process traditionally. However, EBM technology can lower costs and improve production efficiency by manufacturing titanium parts in a vacuum chamber. EBM has advantages such as producing

complex shapes, efficient material use, and fast processing. Ti–6Al–4V alloy is commonly used for EBM production, and efforts have been made to optimize processing parameters for better mechanical properties. Studies on EBM of other titanium alloys, like β -type Ti–24Nb–4Zr–8Sn (Ti2448), have also been conducted. These alloys have a lower Young's modulus, making them suitable for biomedical applications. EBM is a great manufacturing technology for complex parts, but further research is needed to enhance reliability by exploring new titanium alloy powders, improving corrosion resistance, and strengthening mechanical properties [16].

Table 1 Different AM methods and their characteristics [19]

Parameter	Laser Based (eg, SLM)	Electron Beam Based (eg, EBM)	Laser Based Directed Energy Deposition (eg, DMD)
Build envelop	Limited	Limited	Large and flexible
Build capability	Complex geometry, cellular structure, building hollow channels	Complex geometry, cellular structure, building hollow channels	Relatively simpler geometry with less resolution
Beam size	0.1 - 0.5 mm	0.2 - 1 mm	can vary from 2 to 4 mm
Layer thickness	50 - 100 μm	100 μm	500 - 1000 μm
Build rate	<50 cc/h	55 - 80 cc/h	16 - 320 cc/h
Surface finish	Ra 9/12 μm , Rz 35/40 μm	Ra 25/35 μm	Ra 20 - 50 μm , Rz 150 - 300 μm , depends on beam size
Residual stress	High	Minimal	High
Heat treatment	Stress relief required, HIP preferred	Stress relief not required, HIP may or may not be performed	Stress relief required, HIP preferred

Ti–6Al–4V is a titanium alloy that consists of 6 wt.% α stabilizing element Al, 4 wt.% β stabilizing element V, and other interstitial elements like O. The alloy powder used in EBM has a larger specific surface area compared to bulk material, which makes it more susceptible to absorbing impurities from the air. Therefore, strict control of impurity content is necessary to ensure the desired mechanical properties of EBM-produced samples. In Ti–6Al–4V, the tensile strength is mainly influenced by the α stabilizing element Al and the interstitial element O. A study of energy spectra has revealed that Al content decreases during EBM processing due to burning losses of Al. This decrease reduces tensile strength but improves plasticity. Oxygen increases tensile strength, while tensile plasticity is rapidly lost when oxygen content is increased. EBM powders use Ti–6Al–4V powders with an oxygen content of 0.15 wt.% to meet the requirements, below the specified limit of 0.2 wt.% [16].

EBM-produced Ti–6Al–4V parts also benefit from a high oxygen content, which provides improved plasticity in addition to controlling impurity content. A previous study examined EBM-produced Ti–6Al–4V parts, their microstructures, and their mechanical properties. Solid

bulk samples and porous structures have primarily been examined in these studies. The temperature variations during the EBM process, including temperature increase and cooling rate, are complex and differ depending on the shape of the samples and the input energy levels. The phase transformation and microstructure of the Ti–6Al–4V alloy are sensitive to temperature variations, resulting in differences in grain size and shape between solid bulk and porous samples [16].

2.4 Structure and microstructure of Ti alloy obtained via electron beam melting

The use of EBM technology in a vacuum chamber allows for the production of titanium samples with distinct macrostructures and microstructures, resulting in different physical, chemical, and biological properties that can be utilized in various applications. The macrostructure refers to the lattice structure of the sample, which is composed of a unit cell (Fig. 5) [20].

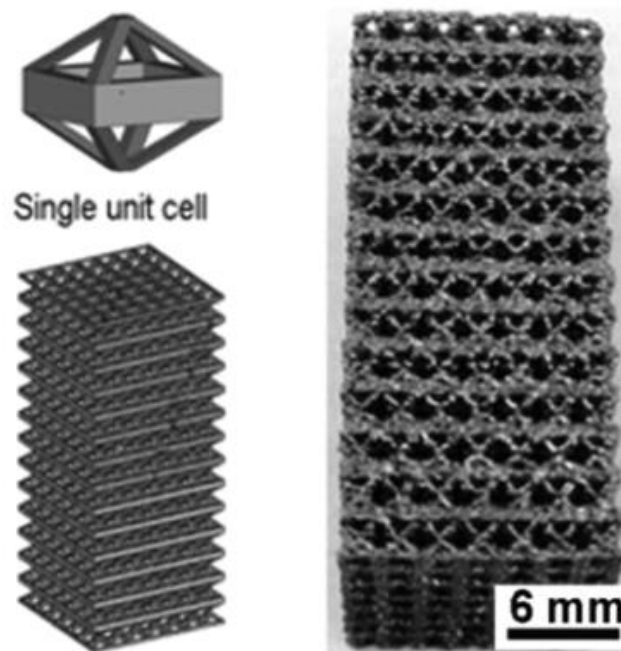


Fig. 5 Design of a structure manufactured by electron beam melting (lattice structure and real manufactured unit cell [20])

Numerous studies have explored the relationship between different unit cells and mechanical properties, although this consideration is only relevant when assuming similar surface roughness and internal defects. One study successfully employed open cubic unit cells to control the lattice structure and create porosity gradients in EBM-manufactured samples, simulating the characteristics and mechanical behavior of human bones with inhomogeneous porosities. However, the presence of surface characteristics and internal defects, such as

incomplete melting of powder particles and orientation of internal pores formed during the melting process, can lead to sample failures during mechanical testing and significantly impact the properties of the manufactured samples. Internal pores can develop between un-melted powder particles due to the trapping of argon or hydrogen during the atomization stage or from the decomposition of absorbed water vapor on the powder surfaces. **Fig. 6a-e** illustrates some common defects that may occur in EBM-manufactured parts [20].

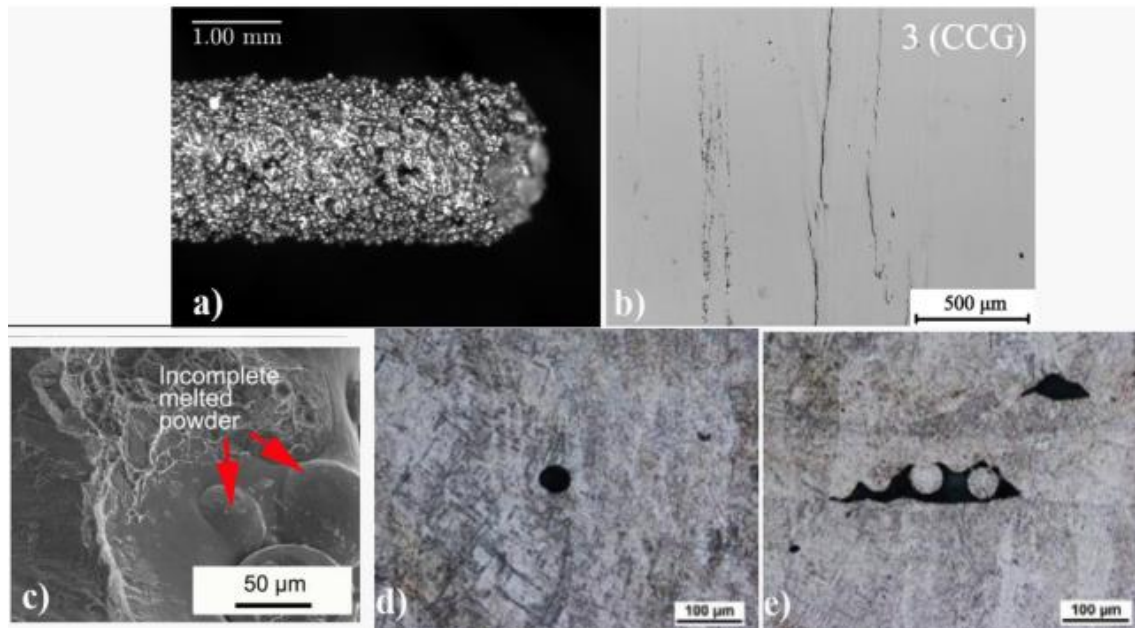


Fig. 6 Possible defects found in parts manufactured by electron beam melting: (a) High surface roughness, (b) cracks, (c) un-melted powder particles, (d) internal pores due to the trapping of gases, and (e) internal porosity between un-melted powder particles [20]

Microstructures play a crucial role in determining the properties of Electron Beam Melting (EBM) manufactured samples. Titanium solidifies in the β phase above a certain temperature, while it remains stable in the α phase at lower temperatures. The transformation between these phases is influenced by the presence of aluminum and vanadium. Different heat treatments and cooling rates during the manufacturing process can result in various microstructures, each with unique properties. Three types of microstructures are typically observed in EBM-produced samples: laminar, equiaxed α grains, and bimodal (equiaxed α grains in a laminar matrix). Each microstructure exhibits different mechanical properties, such as strength, ductility, and fatigue resistance. The cooling rate during EBM affects the phase transformations, with martensitic α' microstructures commonly observed due to the thin struts in lattice structures. Subsequent heat treatments can modify the martensitic structure to achieve a balance between ductility and

resistance. Micrographs of EBM-manufactured samples typically show prior β grains with transformed $\alpha+\beta$ microstructures featuring colony and Widmanstatten morphologies resulting from martensite decomposition [20].

The microstructure of Ti-6Al-4V samples produced by EBM typically consists of ordered lamellae with fine grains, which is expected due to the small melt pool and rapid cooling during the process. The samples contain some α phase at the boundaries of the β grains, which is finer compared to samples obtained by metal casting. XRD analysis revealed that the main constituent of EBM Ti-6Al-4V samples is the α HCP phase, with a small contribution from the β phase. The HCP pattern can be attributed to both the α phase and the α' -martensite, which is spatially smaller than the α -phase platelets. The cast specimen exhibited a typical microstructure consisting of columnar α -crystals. In contrast, no α -case was observed near the surface of the EBM specimens. However, the EBM Ti-6Al-4V prototypes showed α -phase microstructures similar to commercial wrought products, while the mesh and foam prototypes displayed mainly α' -martensitic platelets or mixtures of α and α' platelets, resulting in harder structures and higher strengths. **Fig. 7a-b** provides a comparison of the microstructures of Ti-6Al-4V specimens from EBM and casting, respectively [21].

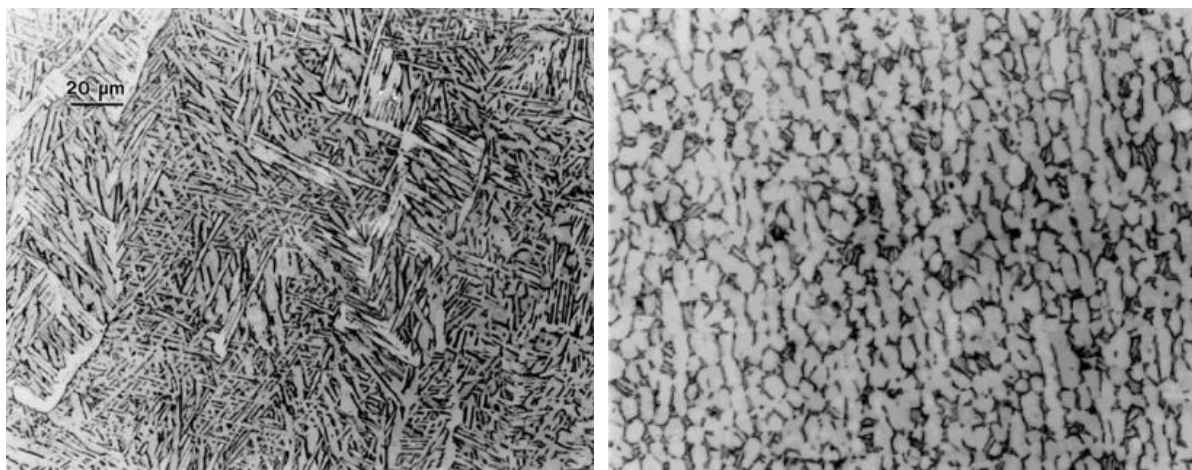


Fig. 7 Microstructures of Ti-6Al-4V specimens made by (a) EBM and (b) casting [21]

During the EBM deposition, each layer undergoes multiple heating and cooling cycles. The peak temperature for each layer gradually decreases, as shown in **Fig. 8**. The cooling process can be divided into three regions: (1) when the peak temperature is above T_{β} (Region A), the α phase transforms into β phase and then back to α phase during cooling; (2) after a few layers, when the peak temperature is below T_{β} (Region B), some α phase lamella transforms into β phase during heating, and new α phase precipitates from the β phase during cooling, while the

remaining α phase coarsens; and (3) when the peak temperature decreases to T_α (Region C), no significant phase transformation occurs, and the microstructures stabilize. This process illustrates how the cyclic thermal treatments affect the evolution of α and β microstructures. The T_β value varies depending on the titanium alloy and can be determined using linear regression analysis as shown in Eq. 2-2 [22]:

$$T_\beta = 882 + 21.1[\text{Al}] - 9.5[\text{Mo}] + 4.2[\text{Sn}] - 6.9[\text{Zr}] - 11.8[\text{V}] - 12.1[\text{Cr}] - 15.4[\text{Fe}] + 23.3[\text{Si}] + 123.0[\text{O}] \quad (2-2)$$

where $[M]$, any element in the equation, represents the weight percent of the element. The Ti-6Al-4V bulk samples displayed a noticeable difference in lath thickness between the top and bottom, attributed to the distinct thermal history of each region. Real-time monitoring of phase evolution during cyclic rapid laser heating of Ti-6Al-4V was achieved through the integration of in situ x-ray diffraction and high-speed imaging. The observations revealed a sequence of transformations from β to α' to β phases, accompanied by changes in lattice strain. These thermal cycles, along with phase transformations, induced element partitioning, lattice defects, and thermal expansion, resulting in a diverse range of microstructures [22].

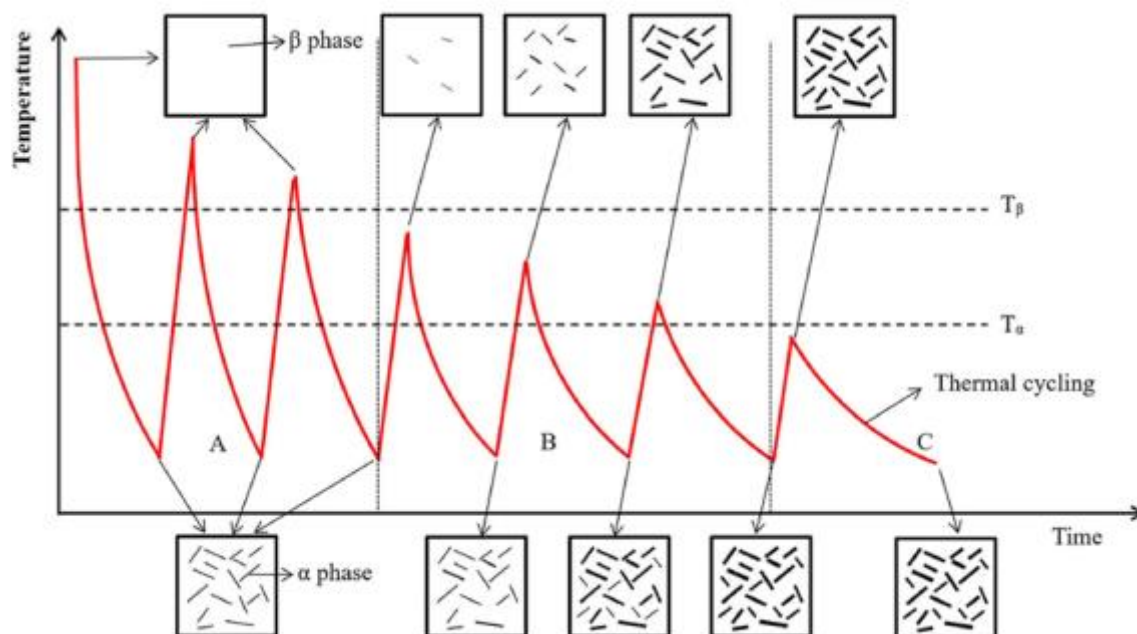


Fig. 8 schematic of thermal cycling and α and β phases evolution [22]

2.5 Biomedical application of EBMed Ti-6Al-4V

Medical device and scaffold 3D printing, also known as additive manufacturing (AM), has become increasingly popular in recent years for tissue engineering, regenerative medicine, and

ex-vivo tissues. Many biomedical devices have received FDA clearance, including ZipDose®, Pharmacoprinting, powder bed fusion, HPAMTM, bio-printer and inkjet printers. Attempts have been made to identify gaps, suggest ideas for future developments, and to emphasize the need of standardization. Researchers at AM are developing a variety of biocompatible materials and processing systems for medical devices such as hips, knees, and articular cartilage joints. The various biomaterials and their application are shown in **Table 2** [23].

Table 2 FDA cleared 3D printed biomedical applications [23]

Material	Application
CP-Ti	Screw and abutment
Ti-6Al-4V	Artificial valve, Stent, Bone fixation
Ti-6Al-7Nb	Crowns, Knee joint, Hip joint
Ti-5Al-2.5Fe	Spinal implant
Ti-15 Zr-4Nb-2Ta-0.2Pd	Crown, Bridges, Dentures, Implants
Ti-29Nb-13Ta-4.6Zr	Crown, Bridges, Dentures, Implants
83%–87%Ti-13%–17%Zr (Roxolid)	Crown, Bridges, Dentures
316L	Knee joint, Hip joint, Surgical tools, Screw
Co-Cr-Mo, Co-Ni-Cr-Mo	Artificial valve, Plates, Bolts, Crowns, Knee joint, Hip joint
NiTi	Catheters, stents
PMMA, PE, PEEK	Dental bridges, articular cartilage, Hip joint femoral surface, Knee Joint bearing surface, Scaffolds
SiO ₂ /CaO/Na ₂ O/P ₂ O ₅	Bones, Dental implants, orthopedic implants
Zirconia	Porous implants, Dental implants
Al ₂ O ₃	Dental implants
Ca ₅ (PO ₄) ₃ (OH)	Implant coating material

In addition, additive manufacturing enables the production of patient-specific implants and prostheses, which can improve surgical outcomes and patient satisfaction. The technology also allows for the use of a wide range of biocompatible materials, including polymers, metals, and ceramics, which can be tailored to the specific needs of the device and the patient. Furthermore, additive manufacturing can facilitate the development of new and innovative designs that were previously impossible to produce using traditional manufacturing techniques. Overall, these advantages make additive manufacturing a promising approach for the production of high-quality and personalized biomedical devices [23].

Due to their capability of producing unlimited designs and complex geometries within short timeframes, AM technologies have been widely used in the medical domain, including implants

and prostheses. As shown in **Fig. 9** AM techniques have been successfully applied to a wide range of medical fields. These include prostheses, implants, surgical instruments, surgery planning and training models, assistive tools, tissue engineering, and artificial organs. EBM and SLM are presented as the most appropriate techniques for manufacturing metallic implants. Unlike other methods, both make it possible to obtain, at low cost, mass implants with complex geometries and in accordance with patients' specific needs. There are, however, some disadvantages associated with these techniques. EBM, for instance, is limited, as it only processes a narrow range of materials given its closed system. These methods also have limitations, such as dimensional precision and powder trapping inside cellular structures. These problems can be solved by reducing the point of the laser or electron beam, which leads to higher precision. EBM and SLM have suffered from these and other limitations, but both techniques are considered most promising in comparison with traditional manufacturing methods to produce implants [20].

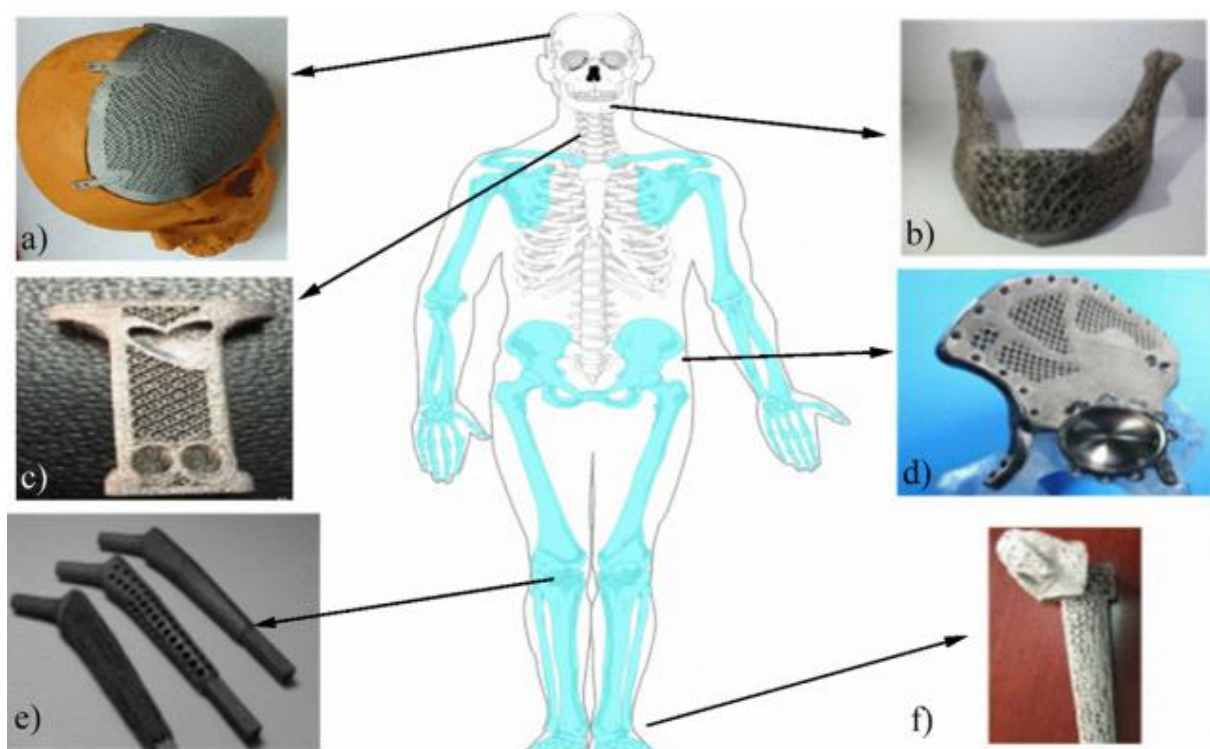


Fig. 9 Ti-6Al-4V alloy implants obtained via electron beam melting: (a) Cranial plate, (b) mandibular prosthesis, (c) cervical vertebral fusion cage, (d) pelvic implant, (e) hip stems, and (f) ankle prosthetics [20]

Currently, one of the most prevalent use of Electron Beam Melting (EBM) technology is in the creation of three-dimensional reconstructions of human skull defects, skull models, porous titanium implants produced using EBM techniques, and titanium implants that are custom-fitted to the skull model. This application is depicted in **Fig. 10** [24].

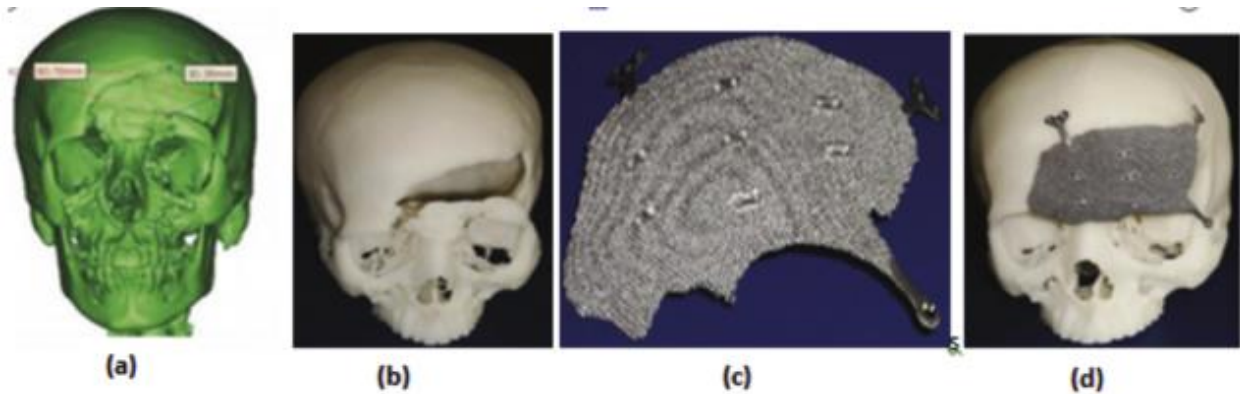


Fig. 10 Representative images of applications of AM in medical sector: (a) 3D digital reconstruction of skull defect. (b) Skull model. (c) Porous Ti implant fabricated with EBM. (d) Model of the skull fitted with a titanium implant [24]

1. Medical devices can benefit from the use of EBM in the following ways:
2. Medical devices requiring tight tolerances and complex geometries require high precision, which EBM can produce.
3. In addition, EBM enables customized medical devices based on the unique anatomy and needs of each patient, such as implants and prostheses.
4. As EBM uses only the amount of material required to create a part, it produces less waste than traditional manufacturing methods. This can result in cost savings and a more sustainable manufacturing process.
5. The parts produced by EBM are durable and strong enough to be used in medical devices that carry loads, such as orthopedic implants.
6. The biocompatibility and corrosion resistance of titanium alloys make them ideal medical device materials [24]–[26].

4. Conclusions

This review paints a clear picture of Electron Beam Melting (EBM) as a transformative force in the biomedical landscape. Its ability to precisely craft complex, high-performance metal components unlocks limitless possibilities for medical implants and devices. We have delved

into the intricacies of EBM technology, scrutinizing its compatibility with diverse biomaterials, process intricacies, microstructure-property relationships, post-processing nuances, and crucial biological interactions. Compared to other AM and traditional manufacturing methods, EBM stands out for its unparalleled proficiency in generating intricate lattice structures and patient-specific implants, tailor-made for individual needs.

However, we acknowledge existing limitations that call for further research and development. Optimizing process parameters, mitigating residual stress, and enhancing surface modification techniques are key areas demanding attention. Yet, the future of EBM shines bright. The emergence of novel materials, groundbreaking multi-material printing capabilities, and the potential for in-situ monitoring during fabrication herald a new era of biocompatible design. By harnessing these advancements, EBM will undoubtedly revolutionize the field of biocompatible implants and medical devices, ultimately improving patient outcomes and shaping the future of healthcare.

This conclusion summarizes the key takeaways of your paper, emphasizes the unique strengths of EBM in the biomedical field, acknowledges limitations and future directions, and ultimately paints an optimistic outlook for the continued evolution of this transformative technology.

References

- [1] R. Kumar, M. Kumar, and J. S. Chohan, "Material-specific properties and applications of additive manufacturing techniques: a comprehensive review," *Bull. Mater. Sci.*, vol. 44, no. 3, p. 181, Sep. 2021, doi: 10.1007/s12034-021-02364-y.
- [2] B. Blakey-Milner *et al.*, "Metal additive manufacturing in aerospace: A review," *Mater. Des.*, vol. 209, p. 110008, Nov. 2021, doi: 10.1016/j.matdes.2021.110008.
- [3] W. E. Frazier, "Metal Additive Manufacturing: A Review," *J. Mater. Eng. Perform.*, vol. 23, no. 6, pp. 1917–1928, Jun. 2014, doi: 10.1007/s11665-014-0958-z.
- [4] M. Yeganeh, M. T. Shoushtari, and P. Jalali, "Evaluation of the corrosion performance of selective laser melted 17-4 precipitation hardening stainless steel in Ringer ' s solution Evaluation of the corrosion performance of selective laser melted 17-4 precipitation hardening stainless steel in Ringer," *J. Laser Appl.*, vol. 042001, no. May, p. 33, 2021, doi: 10.2351/7.0000445.
- [5] M. H. Shaeri Karimi, M. Yeganeh, S. R. Alavi Zaree, and M. Eskandari, "Corrosion

- behavior of 316L stainless steel manufactured by laser powder bed fusion (L-PBF) in an alkaline solution,” *Opt. Laser Technol.*, vol. 138, p. 106918, Jun. 2021, doi: 10.1016/j.optlastec.2021.106918.
- [6] P. Stavropoulos and P. Foteinopoulos, “Modelling of additive manufacturing processes : a review and classification,” *Manuf. Rev.*, vol. 2, no. Manufacturing Rev. Volume 5, 2018, p. 26, 2018, doi: 10.1051/mfreview/2017014.
- [7] J.M.Jafferson and DebduittaChatterjee, “A review on polymeric materials in additive manufacturing,” *Mater. Today Proc.*, vol. 46, no. 2021, pp. 1349–1365, 2021, doi: 10.1016/j.matpr.2021.09.333.
- [8] D. . Pham and R. . Gault, “A comparison of rapid prototyping technologies,” *Int. J. Mach. Tools Manuf.*, vol. 38, no. 10–11, pp. 1257–1287, Oct. 1998, doi: 10.1016/S0890-6955(97)00137-5.
- [9] T. Pereira, J. V Kennedy, and J. Potgieter, “A comparison of traditional manufacturing vs additive manufacturing, the best method for the job,” *Procedia Manuf.*, vol. 30, pp. 11–18, 2019, doi: 10.1016/j.promfg.2019.02.003.
- [10] N. Sabahi, W. Chen, C.-H. Wang, J. J. Kruzic, and X. Li, “A Review on Additive Manufacturing of Shape-Memory Materials for Biomedical Applications,” *JOM*, vol. 72, no. 3, pp. 1229–1253, Mar. 2020, doi: 10.1007/s11837-020-04013-x.
- [11] D. Bourell *et al.*, “Materials for additive manufacturing,” *CIRP Ann.*, vol. 66, no. 2, pp. 659–681, 2017, doi: 10.1016/j.cirp.2017.05.009.
- [12] P. Parandoush and D. Lin, “A review on additive manufacturing of polymer-fiber composites,” *Compos. Struct.*, vol. 182, pp. 36–53, Dec. 2017, doi: 10.1016/j.compstruct.2017.08.088.
- [13] N. Jahangir, M. Arif, H. Mamun, and M. P. Sealy, “A review of additive manufacturing of magnesium alloys A R eview of Additive Manufacturing of Magnesium Alloys,” vol. 030026, 2018, doi: 10.1063/1.5044305.
- [14] W. E. King *et al.*, “Laser powder bed fusion additive manufacturing of metals; physics, computational, and materials challenges,” *Appl. Phys. Rev.*, vol. 2, no. 4, p. 041304, Dec. 2015, doi: 10.1063/1.4937809.
- [15] S. A. Khairallah, A. T. Anderson, A. Rubenchik, and W. E. King, “Laser powder-bed

- fusion additive manufacturing: Physics of complex melt flow and formation mechanisms of pores, spatter, and denudation zones,” *Acta Mater.*, vol. 108, pp. 36–45, Apr. 2016, doi: 10.1016/j.actamat.2016.02.014.
- [16] L. C. Zhang, Y. Liu, S. Li, and Y. Hao, “Additive Manufacturing of Titanium Alloys by Electron Beam Melting: A Review,” *Adv. Eng. Mater.*, vol. 20, no. 5, pp. 1–16, 2018, doi: 10.1002/adem.201700842.
- [17] C. Körner, “Additive manufacturing of metallic components by selective electron beam melting - A review,” *Int. Mater. Rev.*, vol. 61, no. 5, pp. 361–377, 2016, doi: 10.1080/09506608.2016.1176289.
- [18] G. Del, G. Manuela, A. Saboori, P. Fino, and L. Iuliano, “Microstructure and Mechanical Performance of Ti – 6Al – 4V Lattice Structures Manufactured via Electron Beam Melting (EBM): A Review,” *Acta Metall. Sin. (English Lett.)*, vol. 33, pp. 183–203, 2020, doi: 10.1007/s40195-020-00998-1.
- [19] A. Agapovichev, A. Sotov, V. Kokareva, and V. Smelov, “Possibilities and limitations of titanium alloy additive manufacturing,” in *MATEC Web of Conferences*, 2018, pp. 1–8. doi: 10.1051/mateconf/201822401064.
- [20] M. Riascos, C. A. Vargas, and L. M. Baena, “Additive manufacturing of Ti6Al4V alloy via electron beam melting for the development of implants for the biomedical industry,” *Heliyon*, vol. 7, no. 2020, p. e06892, 2021, doi: 10.1016/j.heliyon.2021.e06892.
- [21] X. Gong, T. Anderson, and K. Chou, “Review on Powder-Based Electron Beam Additive Manufacturing Technology,” in *ASME/ISCIE 2012 International Symposium on Flexible Automation*, 2012, pp. 1–9.
- [22] Z. Liu, B. E. I. He, T. Lyu, and Y. U. Zou, “A Review on Additive Manufacturing of Titanium Alloys for Aerospace Applications : Directed Energy Deposition and Beyond Ti-6Al-4V,” *JOM*, vol. 73, pp. 1804–1818, 2021, doi: 10.1007/s11837-021-04670-6.
- [23] S. Singh and S. Ramakrishna, “Biomedical applications of additive manufacturing: Present and future,” *Curr. Opin. Biomed. Eng.*, vol. 2, pp. 105–115, 2017, doi: 10.1016/j.cobme.2017.05.006.
- [24] R. Kumar, M. Kumar, and J. Singh, “The role of additive manufacturing for

- biomedical applications : A critical review,” *J. Manuf. Process.*, vol. 64, pp. 828–850, 2021, doi: 10.1016/j.jmapro.2021.02.022.
- [25] L. E. Murr *et al.*, “Metal Fabrication by Additive Manufacturing Using Laser and Electron Beam Melting Technologies,” *J. Mater. Sci. Technol.*, vol. 28, no. 1, pp. 1–14, 2012, doi: 10.1016/S1005-0302(12)60016-4.
- [26] N. Hrabe, T. Gnäupel-herold, and T. Quinn, “Fatigue Properties of a Titanium Alloy (Ti-6Al-4V) Fabricated Via Electron Beam Melting (EBM): Effects of Internal Defects and Residual Stress,” *Int. J. Fatigue*, vol. 94, pp. 202–210, 2017, doi: 10.1016/j.ijfatigue.2016.04.022.